Full-scale testing of an ultrasonic guided wave based structural health monitoring system for a thermoplastic composite aircraft primary structure

Ochoa, Pedro; Groves, Roger; Benedictus, Rinze

Publication date
2018

Document Version
Final published version

Published in
9th European Workshop on Structural Health Monitoring

Full-scale testing of an ultrasonic guided wave based structural health monitoring system for a thermoplastic composite aircraft primary structure

Pedro Ochôa[1,2], Roger M. Groves[2] and Rinze Benedictus[1]
1 Structural Integrity and Composites Group, Faculty of Aerospace Engineering, Delft University of Technology, The Netherlands
2 Aerospace Non-Destructive Testing Laboratory, Faculty of Aerospace Engineering, Delft University of Technology, The Netherlands

Abstract

This paper describes the test campaign of an ultrasonic guided wave (GW) based structural health monitoring system (SHM) deployed on a full-scale stiffened panel of a thermoplastic composite horizontal stabilizer torsion box. The diagnostic capabilities of the SHM system were successfully evaluated by testing barely-visible impact damage of different severities, applied in different critical areas of the structure. The test campaign allowed the successful validation of a novel procedure to consistently and reliably design a piezoelectric transducer network. It also allowed the gathering of strong evidence that piezoelectric transducer technology has appropriate durability characteristics for real SHM applications. Finally, it enabled the study of the influence of audible structural vibrations on GW signals.

1. Introduction

Structural health monitoring (SHM) is a crucial capability for the implementation of condition-based maintenance programmes for the new generation of large commercial composite aircraft [1-3]. One option for SHM deployment is to monitor critical areas of the primary structure where non-visible damage can jeopardize the capability of sustaining ultimate and fatigue loads. Among the few physical phenomena suitable for this monitoring approach [4,5], ultrasonic guided waves (GW) have a high potential for detailed quantitative diagnostic of damage in thin-walled composite structures [6-8]. The ultrasonic guiding mechanism in plate-like structures makes them sensitive to incipient damage features along the thickness, such as in barely-visible impact damage (BVID) [9] and in delaminations, while propagating across the entire critical area.

One of the main challenges currently facing SHM systems is certification, as it implies the demonstration of mission accomplishment in many different scenarios, with multiple variability factors. Research on SHM reliability [10-13] has shown that computational models are valuable tools that can potentially be used in order to integrate all the meaningful variability factors and to cover the maximum number of possible operational scenarios, while keeping certification costs relatively low. However, computer-based protocols do not eliminate the need for experimental testing. On the contrary, the approximations made in order to create a working model of the entire monitoring environment confirm the existence of knowledge gaps and, thereby, the importance of conducting full-scale testing. Only through component-level and full-scale testing can physical interactions between ultrasonic GW, SHM system and variability factors be fully understood, and model parameters extracted. Furthermore, not all components within an SHM system can be reliably simulated, namely the connectivity of measuring equipment and their integrated operation.

Within the TAPAS project (Thermoplastic Affordable Primary Aircraft Structures), the main goal was to develop technology and corresponding demonstrator products for future large-volume thermoplastic composite applications in primary aircraft structure. This included the integration of SHM technology to enable the development of optimized designs, together with their operation and maintenance for future thermoplastic composite structures.

Therefore, this paper describes all the steps in the test campaign of an ultrasonic GW based SHM system deployed on a full-scale stiffened panel of a thermoplastic composite horizontal stabilizer torsion box. The objectives of the test campaign were to 1) evaluate the performance of the SHM system, 2) increase knowledge about designing a PZT transducer network in a consistent and reliable way, 3) gather more evidence about the actual durability of piezoceramic (PZT) transducers bonded onto a structure subjected to realistic low-energy impacts and high-amplitude LFV, and 4) gain knowledge about the effects of high-amplitude, low-frequency structural vibrations (LFV) on ultrasonic GW signals.

2. Test specimen

One of the structural concepts developed by Fokker Aerostructures B.V. during the TAPAS project was a new horizontal stabilizer torsion box panel entirely made of carbon fibre reinforced polyetherketoneketone (PEKK). The component consisted of a co-consolidated stiffened skin with multiple I-stringers in butt-joint configuration, and two riveted ribs, as depicted in Figure 1. The panel had a maximum length and width of about 2.9 and 1.7 m, respectively, with skin thickness varying between 1.8 and 8.1 mm, and rib thickness between 3 and 3.5 mm.

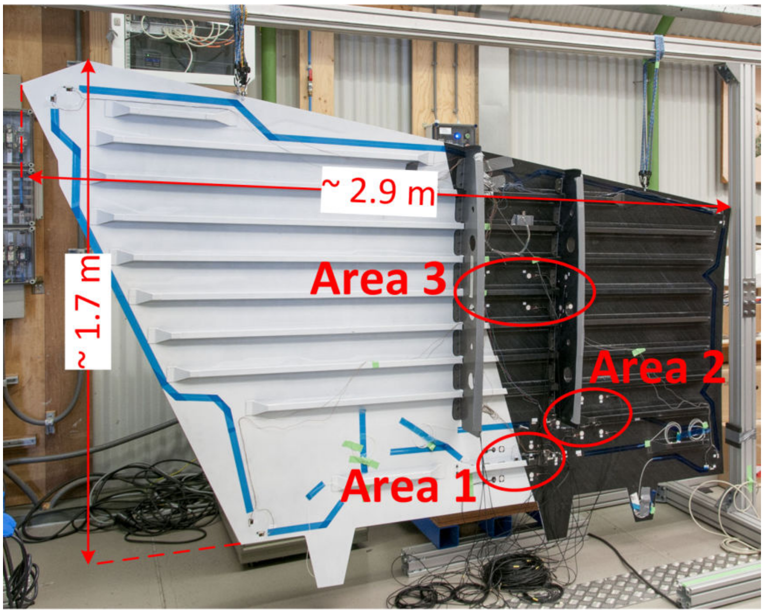

Figure 1. View of the torsion box panel, with main dimensions and selected critical areas.

Among other requirements, the torsion box panel had to be able to withstand a low-energy impact at the outer side of the stringer-skin joint without showing a delamination area larger than 100 mm^2 and without showing visible cracks on the surface of the joint fillet radius. Since it is not possible to visually inspect the joints, and since ultrasonic C-scan is only suitable for detecting stringer-skin delaminations but not cracks in the joint fillet radius, the torsion box was selected as the full-scale test specimen for demonstration of the SHM capabilities in damage diagnostics.

3. Test setup

3.1. Impact damage generation

The impacts were applied by a portable spring-mechanism impactor (see Figure 2) configured to generate the desired nominal impact energy. The projectile head diameter was 12.7 mm and its mass was around 2.7 kg.

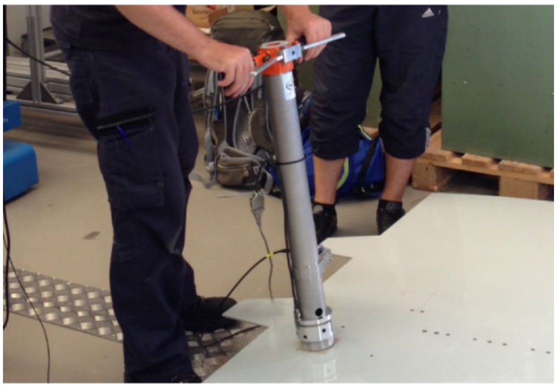

Figure 2. Portable impact gun positioned on the outer side of the skin.

3.2. Guided wave measurements

The equipment used for GW measurements is depicted in Figure 3. The ultrasonic excitation was produced by an Agilent 33500B waveform generator, amplified by a TTi WA301 wideband amplifier and transmitted to the structure by thin PZT actuator discs. The ultrasonic response was sensed by thin PZT sensor discs and acquired by two digital oscilloscopes, PicoScope 4424 and PicoScope 6402A, both connected to a computer.

A novel procedure to consistently design the excitation frequency, geometry and positioning of the PZT transducers was developed based on the optimization of the sensor output, coupled electro-mechanical (EM) response of the transducer-structure assembly, energy transfer of the bonded PZT transducer to the structure, wavefront coverage of the monitored area, and measurement equipment capabilities. The proposed design criteria are not limited to a single damage size, do not resort to unrealistic usage of guided waves (e.g. Lamb mode selection), and are applicable to a generic full-scale composite aircraft primary structure. The application of this novel design procedure resulted in a diameter of 20 mm and a thickness of 0.4 mm. The transducer network configuration for the selected critical areas is shown in Figure 4 and Figure 5. The PZT discs were supplied by APC International Ltd. and were made of APC 850 material.

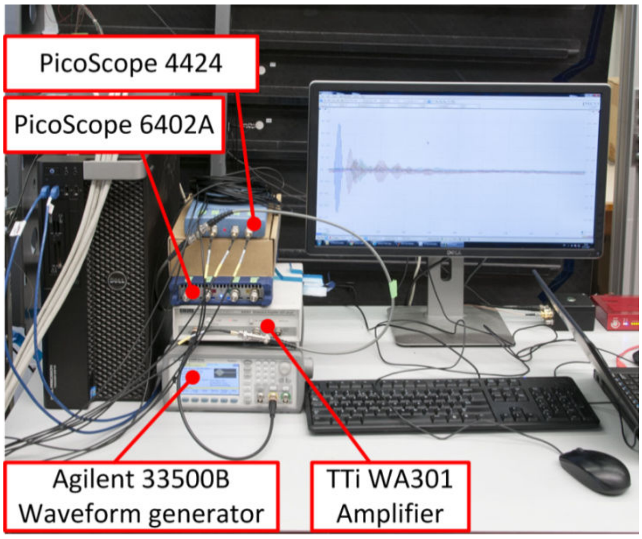

Figure 3. Guided wave measurement setup.

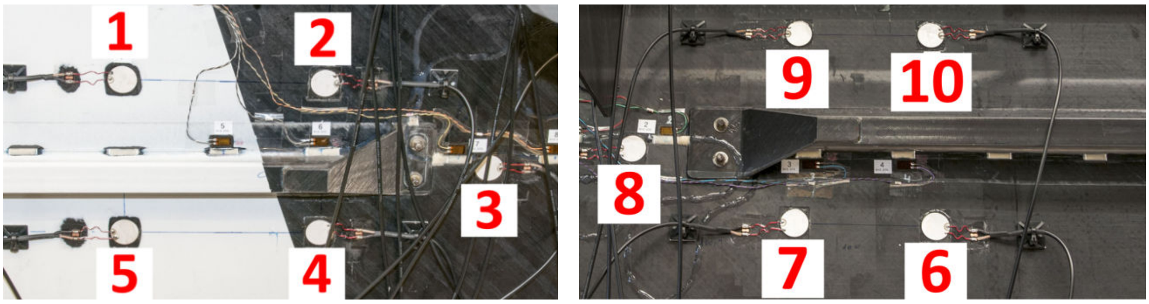

Figure 4. Transducer network on critical area 1 (left) and critical area 2 (right), with transducer identification numbers.

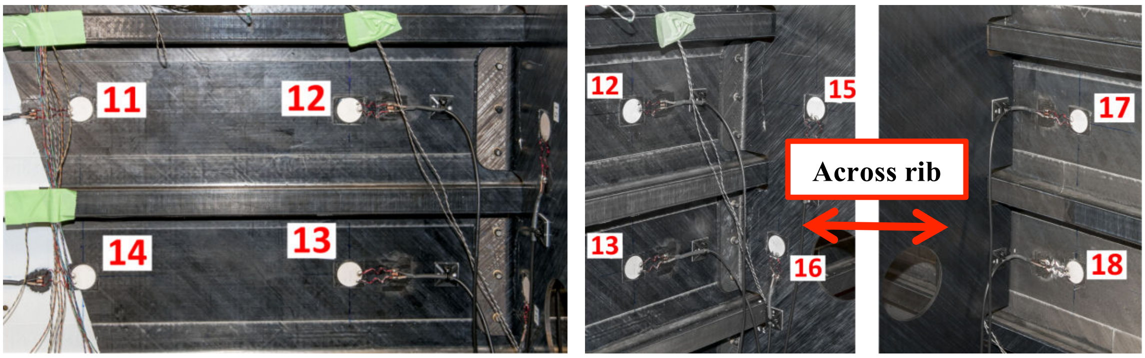

Figure 5. Transducer network on critical area 3, with transducer identification numbers.

3.3. Transducer condition monitoring

The integrity of the transducer network was monitored during the entire test campaign, by measuring the EM susceptance (imaginary part of admittance) of the PZT transducers with a Hioki IM 3570 Impedance analyser connected to Hioki L-2000 4-terminal probe, as shown in Figure 6. The compared evolution of the EM susceptance spectra was used as an indicator of PZT transducer bonding condition and material cracks [14,15].

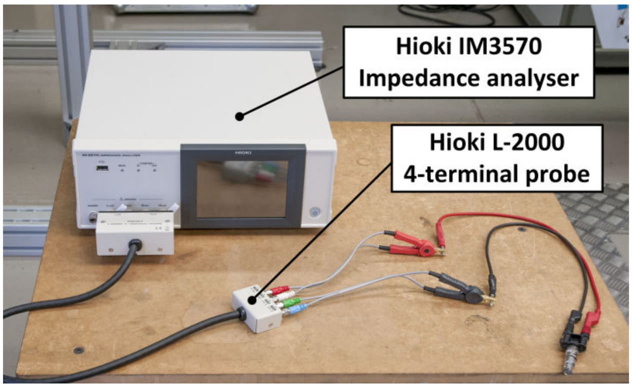

Figure 6. Electro-mechanical susceptance measurement setup.

3.4. Low-frequency vibration

A TIRAvib 50350 mechanical shaker was connected to the torsion box panel (see Figure 7) in order to apply a high-amplitude LFV spectrum. The force signal of the applied LFV was measured by a PCB 208A03 force transducer mounted on the connecting spigot.

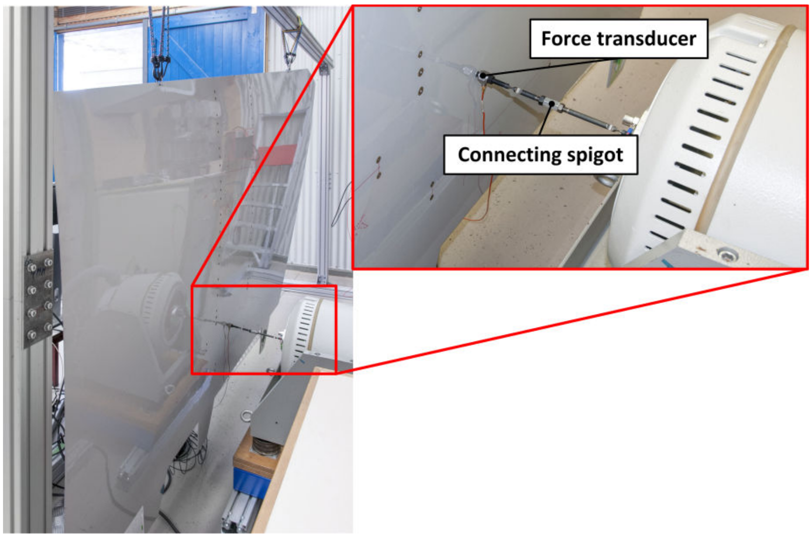

Figure 7. Connection of the mechanical shaker to the torsion box panel.

4. Test procedure

The test campaign took place at the NLR - Netherlands Aerospace Centre during the months of May and June 2017. It consisted of the repetition of the following group of four operations for each structural state.

1) PZT check
2) GW test
3) GW test with LFV
4) PZT check

In total, there were five object states measured: ND, D1, D2, D3 and D3+D3, corresponding to undamaged (or baseline), after impact on area 1, after impact on area 2, after first impact on area 3, and after second impact on area 3, respectively.
The PZT check was always performed for all the 18 PZT transducers. GW tests were conducted on the critical areas, for all possible actuator-sensor combinations, at all the selected excitation frequencies. The operation of GW testing with LFV was performed for only one actuator-sensor combination within a critical area. The goal of adding a step of GW testing with LFV was to study LFV effects on GW propagation and the subsequent damage diagnostic performance. Having a PZT check as 1^{st} and 4^{th} operation had the purpose of assessing the effect of LFV on the transducer network integrity.
In addition to the standard *intra*-area GW tests, *inter*-area GW tests were performed with PZT01 as an actuator and PZT07, PZT10, PZT11 and PZT 18 as sensors, in order to evaluate the capability of detecting damage accumulation across all three critical areas.

4.1. PZT checks

The EM susceptance of the PZT transducers was always measured between 50 and 500 kHz, with steps of approximately 0.56 kHz.

4.2. GW tests

The ultrasonic GW tests were performed at three different nominal excitation frequencies: 123, 213, 335 kHz for areas 1 and 2; 112, 198, 350 kHz for area 3. The excitation pulse was a sinusoidal tone-burst with the amplitude modulated by a Hanning window. Ten sinusoidal cycles per pulse were used for areas 1 and 2, and five for area 3. The nominal excitation frequencies and the number of pulses cycles were selected based on the optimization of sensor output and coupled EM transducer response according to the novel procedure for transducer network design summarised in Section 3.2. The waveform generator was set to send an excitation pulse every 10 ms.

4.3. GW tests with LFV

In this case the procedure for the GW signal acquisition was exactly the same as the one described in subsection 4.2. The difference was the simultaneous application of a high-amplitude LFV spectrum with frequency randomly varying between 20Hz and 2000 Hz, amplitude randomly varying between 5 and 10 G_{RMS}, and duration of approximately 5 minutes.

4.4. Impact application

To clarify the impact location description, Figure 8 shows relevant reference directions on the torsion box panel. The structure was impacted at the stringer locations on the outer side of the skin, at the locations listed in Table 1 and shown in Figure 9. The impact gun was configured to generate a nominal impact energy of 50 J. For the second impact on area 3 the nominal energy was 30 J.

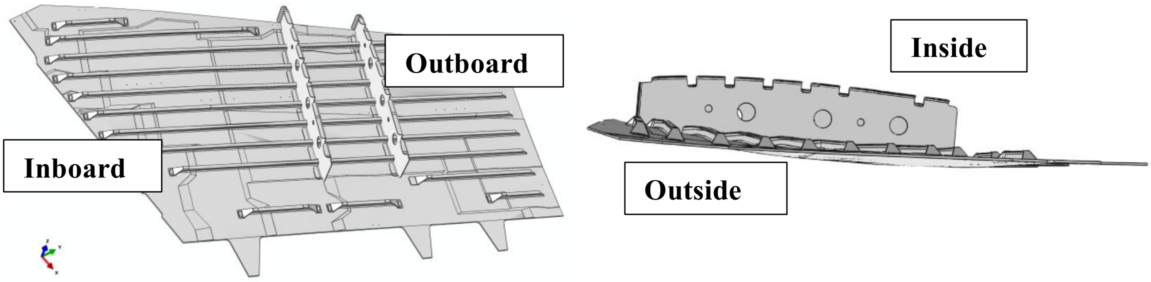

Figure 8. Reference directions for the torsion box panel.

Table 1. Impact locations along the stringers.

Abbreviation	Impact location
Impact location 1 (IL 1)	100 mm from stringer run-out
Impact location 2 (IL 2)	100 mm from stringer run-out
Impact location 3 (IL 3)	100 mm away from outboard rib

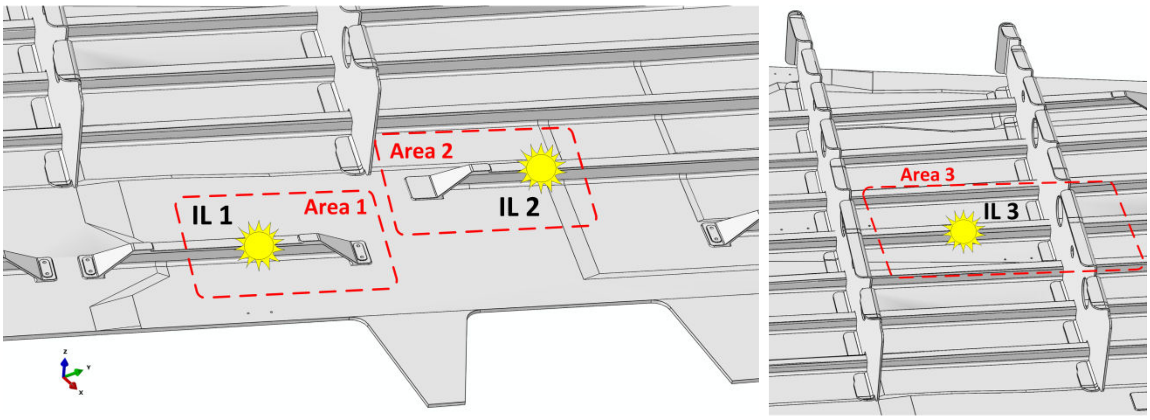

Figure 9. Detailed views of the inside of critical areas 1 and 2 (left), and critical area 3 (right), with the corresponding impacts locations (IL). The impacts were performed on the outside of the skin.

4.5. Experimental limitations

The amplifier used for the excitation signal had a wide frequency band, which introduced non-linearity and parasitic frequencies in the signal if the amplification factor was higher than 1.6. Therefore, it was decided not go beyond this value, thereby limiting the excitation signal amplitude to 16 Vpp.
The GW tests with LFV could only be performed with the PicoScope 4424, because that was the only digital oscilloscope with an amplitude range high enough to capture the voltages induced by the LFV. Consequently, there were only four channels available, which meant that only one actuator and three sensors could be connected.

4.6. Setbacks during testing

During the test campaign there were some setup and time constraints which resulted in the setbacks below. Nevertheless, these did not compromise any of the objectives of the test campaign.

a) GW tests with LFV were not performed for area 3.
b) GW tests with LFV for area 1 were only performed at 123 kHz
c) Impact on area 1 had to be performed right after second impact on area 3, preventing any testing in between the two occurrences.
d) GW tests with sparse transducer network were not performed for the baseline.
e) GW tests with sparse transducer network were only performed at one excitation frequency

5. Test results

The filtered GW signals were used to compute the frequency-domain root-mean-square error, as defined in Equation (1), where $s(f)^0$ and $s(f)$ are the frequency-domain baseline and new-state signals, respectively, and n is the number of signal sample points.

$$RMSE_f = \sqrt{\frac{\sum_{i=1}^{n}\left[s(f)_i - s(f)_i^0\right]^2}{\sum_{i=1}^{n}\left[s(f)_i^0\right]^2}} \tag{1}$$

The multi-path unit-cell network concept described in [16,17] was then applied and the final damage index (DI) value for a monitored area was computed as the weighted-average of all paths in that area, where the weighting factor for each path p of a total N is defined by Equation (2), and the final DI value by Equation (3). The application of this concept makes the DI independent of propagation path orientation with respect to the structural elements in the monitored area, thereby generating a DI value which corresponds to a measure of the total change in the scatter field.

$$w_p = \frac{RMSE_{f,p}}{\sum_{p=1}^{p=N} RMSE_{f,p}} \tag{2}$$

$$DI = \sum_{p=1}^{p=N} w_p RMSE_{f,p} \tag{3}$$

All the different BVID were detected (see Figure 10). The DI values for the largest damages (D3 and D3+D3) were comparable to the values for similar damage size obtained by Monnier [18], thereby confirming the accuracy of damage quantification. However, contrary to previous research [19], the SHM system was equally sensitive to both large and small BVID (D1 and D2). In fact, the DI values for Area 1 allowed a less ambiguous diagnostic than that performed by ultrasonic C-scan.

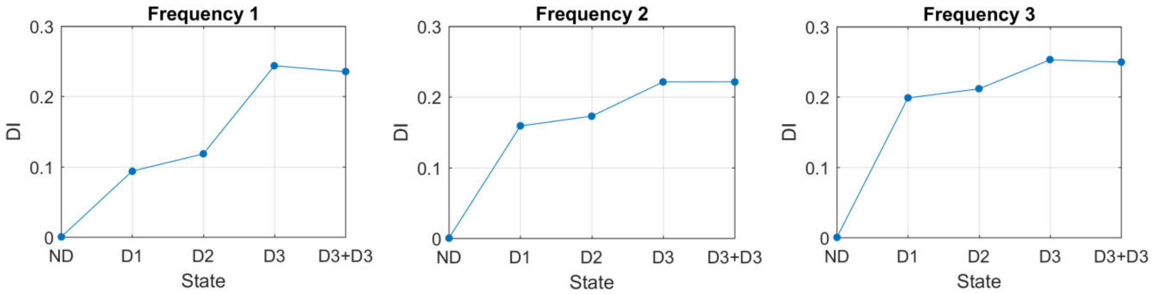

Figure 10. Damage index for each state at each tested frequency.

Additionally, the accumulation of successive BVID was detected and quantified using a sparse transducer network, without requiring a transducer placement optimization for each difference damage scenario (see Figure 11).

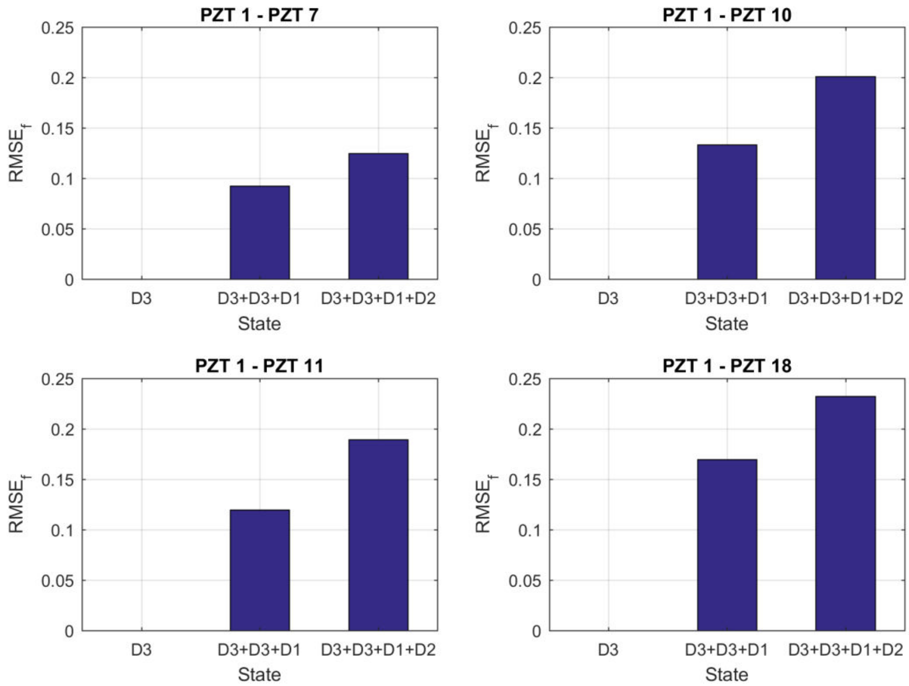

Figure 11. Damage index for sparse transducer network.

The aforementioned observed diagnostic capabilities successfully validated the novel procedure to consistently define the excitation frequency, geometry and positioning of the piezoelectric (PZT) transducers, as described in Section 3.2. The novel procedure is not limited to a single damage size, does not resort to GW mode selection, and is applicable to a generic full-scale composite aircraft primary structure.

The impact points and the LFV application point were in the close vicinity of the transducer locations. These circumstances could potentially lead to damage in the transducer network, either by cracking of the PZT material or by partial disbonding of the transducer. The time evolution of the coefficient of correlation between each EM susceptance curve (B_1) and the one at the start (B_0) (see Figure 12), as computed by Equation (4), showed that the integrity of the PZT transducers barely varied throughout the entire test campaign, after all the impacts and high-amplitude LFV. This brought extra confidence in the SHM results and constitutes strong evidence that PZT transducer technology has appropriate durability characteristics for SHM. Moreover, it also shows that transducer network condition monitoring can be readily integrated in the SHM diagnostic functions.

$$DI_{PZT} = 1 - CorrCoef\left(B_0, B_1\right) \tag{4}$$

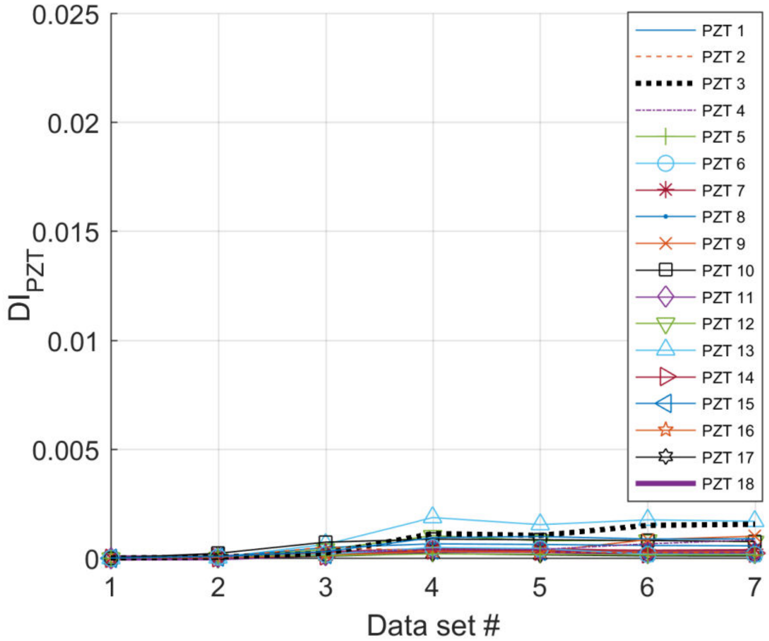

Figure 12. Evolution of the transducer network condition during the test campaign.

Finally, the study about the effects of high-amplitude LFV on ultrasonic GW signals was initiated, revealing the presence of coherent noise in the filtered signals (see Figure 13). This coherent noise has been interpreted as the result of the superposition of multiple dispersive wave groups produced by mode conversion at the moment of reflection on the corrugated panel surface. Although the investigation is still ongoing, there is strong evidence supporting the hypothesis that it might be possible to analyse LFV effects on GW signals under the assumption of a permanently corrugated structure subjected to static stress.

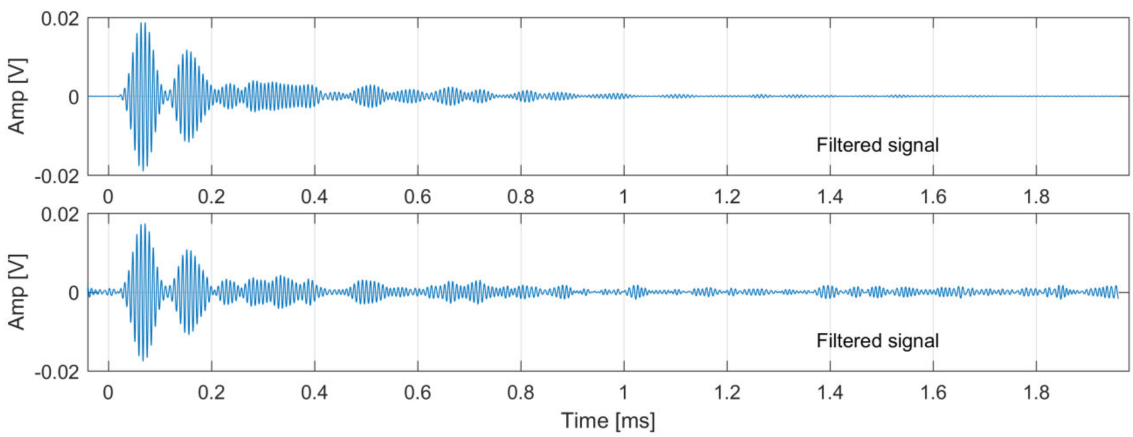

Figure 13. Filtered signal without LFV (top) and with LFV (bottom).

6. Conclusions

This paper describes the test campaign of an ultrasonic guided wave (GW) based structural health monitoring (SHM) system deployed on a full-scale stiffened panel of a thermoplastic composite horizontal stabilizer torsion box developed within the TAPAS project. The full-scale panel provided realistic material and geometric complexity, as well as realistic damage and vibration conditions which were vital for evaluating the performance of the SHM system, and for studying physical interactions between ultrasonic GW, the SHM system and variability factors.

The contribution to the TAPAS project was successfully accomplished by demonstrating the barely-visible impact damage (BVID) diagnostic capabilities of the ultrasonic GW based SHM system. More specifically, 1) the SHM system accurately detected all the BVID cases, thereby 2) validating a novel procedure for designing a piezoceramic (PZT) transducer network in a consistent and reliable way. Additionally, 3) the realistic low-energy impacts and high-amplitude low-frequency vibration (LFV) barely affected the integrity of the PZT transducers throughout the entire test campaign, which constitutes strong evidence that bonded PZT transducers have appropriate durability for SHM. Finally, 4) it was possible to start understanding the effects of high-amplitude LFV on ultrasonic GW propagation, as there was coherent noise was consistently observed in the signals.

The knowledge gained from these studies contributes to improving the reliability of ultrasonic GW based SHM systems. This proves that rather than just being an auxiliary step in validating computer models, full-scale testing should be employed in order to gain knowledge about physical interactions that are crucial to fulfil SHM certification requirements.

Acknowledgements

This research is part of the Thermoplastic Affordable Primary Aircraft Structure 2 (TAPAS 2) project, financed by the Netherlands Enterprise Agency of the Ministry of Economic Affairs.

The authors would like to thank Frank Grooteman from the NLR - Netherlands Aerospace Centre for his collaboration before, during and after the test campaign on the torsion box panel, and Pieter Lantermans from Fokker Aerostructures B.V. for providing the torsion box panel. Last but not least, the authors would like to show their gratitude to Lourens Prikken and Dion Baptista, also from the NLR, for their support during the installation of the piezoelectric transducers on the torsion box panel.

References

1. L Wenk and C Bockenheimer, “Structural health monitoring: a real-time on board ‘stethoscope’ for condition-based maintenance”, Airbus Technical Magazine - Flight Airworthiness Support Technology, August 2014, p. 22.
2. G Gardiner, “Structural health monitoring: NDT-integrated aerostructures enter service”, CompositesWorld, July 31, 2015.
3. RA Smith, “NDT and SHM Requirements for Aerospace Composites”, Report from the Aerospace Workshop, BINDT, UK, February 2016.

4. AJ Croxford, PD Wilcox, W Drinkwater and G Konstantinidis, "Strategies for guided-wave structural health monitoring", Proc. R. Soc. A 463, pp 2961-2981, 2007.
5. V Giurgiutiu, "Structural health monitoring with piezoelectric wafer active sensors", 2nd ed. Academic Press – Elsevier, 2014.
6. Z Su, L Ye and Y Lu, "Guided Lamb waves for identification of damage in composite structures: A review", J. Sound Vib. 295, pp 753-780, 2006.
7. Z Su and L Ye, "Identification of damage using Lamb waves: from fundamentals to applications", Springer, 2009.
8. M Mitra and S Gopalakrishnan, "Guided wave based structural health monitoring: A review", Smart Mater. Struct. 25(053001), pp 1-27, 2016.
9. P Ochôa, V Infante, JM Silva and RM Groves, "Detection of multiple low-energy impact damage in composite plates using Lamb wave techniques", Compos. B 80, pp 291-298, 2015.
10. RB Thompson, "A unified approach to the model-assisted determination of probability of detection", AIP Conf. Proc. 975, pp 1685-1692, 2008.
11. JC Aldrin, EA Medina, EA Lindgren, C Buynak, G Steffes and M Derriso, "Model-assisted probabilistic reliability assessment for structural health monitoring systems", AIP Conf. Proc. 1211, pp 1965-1972, 2010.
12. JC Aldrin, EA Medina, EA Lindgren, CF Buynak and JS Knopp, "Case studies for model-assisted probabilistic reliability assessment for structural health monitoring systems", AIP Conf. Proc. 1335, pp 1589-1596, 2011.
13. P Ochôa, RM Groves and R Benedictus, "Reliability analysis of an ultrasonic guided wave based structural health monitoring system for a carbon fibre reinforced thermoplastic torsion-box", Proc. 11th IWSHM, September 12-14, 2017, Palo Alto, CA, USA, pp 3059-3068, DEStech Publications, Inc.
14. I Buethe, M Moix-Bonet, P Wierach and CP Fritzen, "Check of piezoelectric transducers using the electro-mechanical impedance", Proc. 7th EWSHM, July 8-11, 2014, Nantes, France, pp 748-755, Curran Associates, Inc.
15. G Park, CR Farrar, FL di Scalea and S Coccia, "Performance assessment and validation of piezoelectric active-sensors in structural health monitoring", Smart Mater. Struct. 15, pp 1673-1683, 2006.
16. V Janapati, SK Yadav, A Kumar, R Ikegami and E Habtour, "Fatigue crack quantification approach based on multi-path unit-cell concept in sensor network", Proc. 8th EWSHM, July 5-8, 2016, Bilbao, Spain, pp 150-159, Curran Associates, Inc.
17. SK Yadav, H Chung, F Kopsaftopoulos and FK Chang, "Damage quantification of active sensing acousto-ultrasound-based SHM based on a multi-path unit-cell approach", Proc. 11th IWSHM, September 12-14, 2017, Palo Alto, CA, USA, pp 3093-3103, DEStech Publications, Inc.
18. T Monnier, "Lamb waves-based impact damage monitoring of a stiffened aircraft panel using piezoelectric transducers", J. Intell. Mater. Syst. Struct. 17, pp 411-421, 2006.
19. B Eckstein, MM Bonet, M Bach and CP Fritzen, "Lamb wave interaction at debondings due to impact damage in complex stiffened CFRP structures", Proc. SPIE 10170(101701Q), pp 1-14, 2017.